Mechanical Systems and Signal Processing 141 (2020) 106625

Contents lists available at ScienceDirect

Mechanical Systems and Signal Processing

journal homepage: www.elsevier.com/locate/ymssp

Application of neural network algorithm in fault diagnosis of mechanical intelligence

Xianzhen Xu [a,1], Dan Cao [b,1], Yu Zhou [a], Jun Gao [c]

[a] College of Chemistry and Chemical Engineering, Shandong Sino-Japanese Center for Collaborative Research of Carbon Nanomaterials, Collaborative Innovation Center for Marine Biomass Fiber Materials and Textiles, Laboratory of Fiber Materials and Modern Textile, Qingdao University, Qingdao 266071, China
[b] College of Engineering, Ocean University of China, Qingdao 266100, China
[c] College of Chemical and Environmental Engineering, Shandong University of Science and Technology, Qingdao 266590, China

ARTICLE INFO

Article history:
Received 26 September 2019
Received in revised form 13 December 2019
Accepted 5 January 2020
Available online 25 January 2020

Keywords:
Neural network
BP neural network
Fuzzy neural network
Intelligent fault detection

ABSTRACT

In recent years, mechanical fault diagnosis technology at home and abroad has developed rapidly, and its application has spread to various industrial fields. Due to the complex structure of rotating machinery, the ambiguity and complexity of fault characteristics and causes are common, and it is difficult to carry out fault diagnosis. Although many researches have been carried out and some research results have been obtained, the overall diagnostic level is not very high. High, which is extremely inconsistent with the status quo that is widely used in production. Therefore, it is of great significance to carry out fault diagnosis research on rotating machinery. In this paper, this paper briefly introduces the research and application of intelligent technology in equipment fault diagnosis, and gives the superiority of fuzzy neural network technology application in equipment fault diagnosis, and expounds the basics of fuzzy theory and neural network technology. Based on the principle, the advantages and disadvantages of the two in fault diagnosis are analyzed, and the necessity of combining the two is explained. Based on the previous research on the combination of fuzzy theory and neural network, a new combination method is proposed, and a fuzzy neural network model suitable for fault diagnosis is established. A fuzzy inference method based on fuzzy network is constructed, which realizes the knowledge of information through the extraction, optimization and screening of fuzzy rules. At the same time, the fuzzy neural network learning weights are transformed into case-based reasoning-based diagnostic guidance operators, which play an important role in the rapid extraction of knowledge and improve the diagnostic accuracy. The experimental results show that compared with the commonly used neural network and fuzzy theory fault diagnosis methods, this method can make up for the shortcomings of fuzzy theory and neural network alone. It has higher diagnostic accuracy and has a good application prospect in the field of rotating machinery fault diagnosis.

1. Introduction

With the development of industrial production and science and technology, a clear trend in the development of modern mechanical equipment is the development of large-scale, high-speed, continuous and automated. The structure is becoming

[1] Xianzhen Xu and Dan Cao contributed equally to this work.

E-mail addresses: xuxianzhen@qdu.edu.cn (X. Xu), zhouyu@qdu.edu.cn (Y. Zhou), gao@sdust.edu.cn (J. Gao)

https://doi.org/10.1016/j.ymssp.2020.106625
0888-3270/

more and more complex, the level of automation is correspondingly increased, and the production efficiency is getting higher and higher. This is a positive side. However, in the event of failure of these devices, it will affect the operation of the entire system. Not only will the equipment be greatly damaged, but also cause direct or indirect huge economic losses to people, and even pose a great threat to people's lives and lives. Sometimes the consequences are unimaginable. In order to enable these devices to operate normally and efficiently, to create more value for enterprises and society, and to reduce the economic losses caused by failures in the production process and to avoid the occurrence of malignant accidents, equipment condition monitoring and fault diagnosis technology [1,2] came into being. Since the 1970s, some countries with advanced technology have begun to adopt fault diagnosis methods. Using fault diagnosis to obtain the actual state of the equipment, and then determining whether it is necessary to repair according to the actual state of the equipment, as well as the location and time of repair, has been applied in many different fields of the country, using fault diagnosis technology to reduce the fault and save a huge manpower and material resources. According to estimates by a foreign authority, a 400Mw capacity steam turbine generator set. If the failure diagnosis technology can reduce the planned shutdown rate and the failure forced shutdown rate by 1%, it can save $17 million in maintenance costs in one year. Nowadays, with the in-depth research and extensive application of intelligent technology, fault diagnosis technology has entered a new stage of development—developing rapidly towards diversity and intelligence. This discipline has obvious scientific, applied and cross-cutting characteristics; it has technical strategies such as zeroing out, gathering zeros into layers, deepening layers, and comprehensive evaluation; combining analysis and synthesis, combining qualitative analysis with quantitative analysis, the combination of mechanism analysis and logic analysis, the basic thinking method combining hypothesis and verification. It has become one of the hot research directions in the field of mechanical equipment fault diagnosis at home and abroad.

There is no uniform definition of the definition of mechanical equipment failure, and the definitions in various documents are not the same. From the point of view of fault diagnosis, a popular saying is that the mechanical equipment is abnormal during operation and cannot meet the predetermined performance requirements. Or the parameter that characterizes its performance exceeds a certain limit, which may cause some or all of the equipment to lose its function. Mechanical faults can be classified from different angles. Different classification methods reflect different aspects of mechanical faults. The purpose of classifying mechanical faults is to better take corresponding countermeasures for different fault forms. The various fault classification methods are as follows: (1) Classified according to the cause of the failure: deterioration failure; human failure. (2) Classified by fault duration: temporary fault; persistent fault. (3) According to the fault formation speed: sudden failure; gradual failure. (4) Classified according to the nature of the fault: functional faulty equipment; parameter faulty equipment. (5) Classified by fault hazard: catastrophic failure; general failure. (6) Classification according to whether the fault occurred: actual fault; potential fault. In actual production and life, most of the mechanical equipment is a rotating machine. The main function of the rotating machine is done by the rotating action, and the rotor is its main component. An important feature of the failure of a rotating machine is that the machine is accompanied by abnormal vibration and noise, and the vibration signal of the rotor is analyzed for the research object. Common faults that cause abnormal vibration of the rotor are unbalanced, misaligned, loose bearing housing, radial friction of the rotor, and oil film whirl.

A neural network [3–5] is a network of simple (usually adaptive) components and their hierarchically organized massively parallel structures that deal with the realities of the real world in the same way as the biological nervous system [6,7]. Artificial neural network is an information processing system [8] composed of the structure and function of physiological human brain neural network and some theoretical abstraction, simplification and simulation of several basic characteristics. The structural model of an artificial neuron can be represented as a node. Where θ is the threshold, $f(X, W)$ is the activation function of the node, $X = (x_1, x_2, \cdots x_n)^T$ is the input vector, and W is the parameter vector indicating the strength of the connection between the neurons (ie, each input Weights can be adjusted during the learning process. Multiple such points are connected into a directed graph to form an adaptive neural network. The information processing of artificial neurons is divided into three parts. First, the inner product of the input signal and the strength of the neuron connection is completed, and then the result is passed through the activation function and then judged by the threshold function. If it is greater than the threshold, the nerve is the element is activated, otherwise it is in a suppressed state. In this way, artificial neurons are very similar to biological neurons. In general, the neural network model is determined by three factors: the topology of the network, the characteristics of the neurons, and the learning or training rules. The topology of neural networks can be divided into hierarchical network models and interconnected network models. The former divides the neurons into several layers, and the layers are sequentially connected. The input of the layer I is only associated with the output of the layer $I-1$. The latter allows for the interconnection of any two neurons. There are also some networks that are a mixture of the two. The characteristic function of a neuron is a composite function of an activation function [9,10] and a threshold function, usually using a step function and a Sigmoid function [11,12]. Neural network learning algorithms can be divided into two categories: supervised and unsupervised learning algorithms. A supervised learning algorithm requires both input and correct output. The network adjusts the network based on the difference between the current output and the desired target output, so that the network can respond correctly. The unsupervised learning algorithm only needs to give a set of inputs, and the network can obtain an output from the input of the same class through learning.

China's fault diagnosis technology started in the late 1970s, and this period from 1983 to 1985 was called the "learning start stage" of equipment fault diagnosis in China. Many industries, enterprises and research institutes all over the country have begun to learn from foreign experience, conduct domestic research, formulate implementation rules, raise development funds and carry out pilot work, so that the research on the theory and methods of equipment diagnostic technology and the

promotion of practical applications are gradually listed. Into the agenda of equipment management. From 1985 to 1989, it was the stage of implementation and popularization of equipment diagnostic technology in China. During this period, the role of diagnostic technology was not limited to promoting the reform of maintenance methods and modernization of equipment management, but also to prevent equipment accidents, maintain safe production, and save maintenance. An important means of reducing costs, reducing energy consumption, improving product quality and strengthening environmental protection. After entering the 1990s, diagnostic technology entered a stage of combining popularization and improvement. Its main symbol is the development of data acquisition and computer-aided diagnosis technology. The former is an important means to widely develop and popularize diagnostic techniques, while the latter is moving toward high. The only way to diagnose horizontally. At present, research on domestic diagnostic techniques focuses on the following aspects: (1) The development of sensor technology. Like eddy current sensors, speed sensors, acceleration sensors, etc., they have already reached the international lead, but there is still a certain gap in stability and reliability, which is also one of the future efforts. (2) Research on signal analysis and processing techniques. From the traditional spectrum analysis and time domain analysis, some advanced technologies, such as frequency domain analysis Fourier transform and wavelet analysis, have been introduced. (3) Research on artificial intelligence, expert systems, and neural networks. With the rapid development of computers, research in this area has become the mainstream of fault diagnosis development. Many domestic research institutions have also done a lot of work, but this technology is far from the level expected by people, and the progress is relatively slow. (4) About the development and research of diagnostic systems. From the stand-alone inspection and diagnosis of the era to the master-slave structure of the upper and lower machines, to today's network-based distributed structure. The system is more and more complex and the real-time performance is getting higher and higher.

This thesis mainly studies the method of fault diagnosis of rotating machinery based on artificial neural network. Artificial neural network has a good function of pattern classification [13–15] and has a very wide application prospect in the field of mechanical fault diagnosis. For the characteristics of fault diagnosis, by analyzing the characteristics of the vibration signal, it is possible to diagnose the internal fault of the device relatively accurately. Therefore, the fault diagnosis of rotating machinery in this thesis is mainly based on the analysis of vibration signals. According to experimental research, the paper first selects a three-layer neural network for analysis. The input to the neural network is eight typical fault feature vectors, and the outputs represent misalignment faults, unbalance faults, rub-impact faults, and vortex four faults. Through the training and learning of the neural network, the purpose of identifying and classifying faults is achieved. In order to further improve the accuracy of the neural network, this paper combines the fuzzy theory with the neural network to improve the accuracy of fault recognition by fuzzifying the eigenvectors of the input and output.

2. Proposed method

2.1. BP neural network algorithm

(1) Structure of BP neural network and its mathematical description

The perceptron's excitation function [16–18] uses a symbol threshold unit, so that the output of the neural network has only two cases. In the BP neural network [19,20], the excitation function utilizes a nonlinear function, and the network structure employs a multi-layer neural network, which makes the application of the BP neural network more extensive. In general, the multi-layer neural network consists of an input layer, a hidden layer [21,22], and an output layer. The number of neurons in each layer is different, and the excitation function used may be different.

Let I_{jk} denote an input value of a node that is propagated to the first layer after an input vector X_k is input into the network. O_{jk} represents the output value of the layer 1 at node j. $W_{ij}^{(l-1)}$ is a weight of the layer 1 node j to which a node i of the first $l-1$ layer is connected. $n^{(l-1)}$ describes the number of nodes in the $l-1$th layer. f is a transfer function of the node neuron. Here the neuron transfer function can usually use a differentiable Sigmoid type function. The relationship between input and output between them is as follows:

$$I_{jk}^{l} = \sum_{i=1}^{n^{(l-1)}} W_{ij}^{l-1} O_{ik}^{l-1} \tag{1}$$

$$O_{jk}^{(l)} = f\left(I_{jk}^{(l)}\right) \tag{2}$$

Then an expected output value of instance k for node j is ${O_{jk}}^{*(l)}$, and the error between this node j and a network calculation output value ${O_{jk}}^{(l)}$ for instance k can be defined as follows:

$$E_{jk}^{(l)} = \frac{1}{2}\left(O_{jk}^{*(l)} - O_{jk}^{(l)}\right)^2 \tag{3}$$

Assuming that the first layer is an output layer of the BP neural network, then the node j is an output node, then there are: ${O_{jk}}^{*(l)} = {y_{jk}}^{*}$, ${O_{jk}}^{(l)} = y_{jk}$, and an output error of the instance k is expressed as:

$$E_{jk}^{(l)} = \frac{1}{2}\left(y_{jk}^{*(l)} - y_{jk}\right)^2 \tag{4}$$

Suppose that any of the N instances of the n instances of the k output nodes in the output layer can compute the output of each of the m expected outputs of the instance k, i.e. $E_{jk}{}^{(l)} \leqslant \varepsilon, j = 1, 2, \cdots m$, that means the end of the learning process. ε indicates the specified allowable error range. Otherwise, the weight distribution W is modified during the back propagation of the error. Modifying this weight according to a negative gradient function of its error is:

$$\begin{cases} W_{ij}^{(l-1)} = W_{ij}^{(l-1)} + \Delta W_{ij}^{(l-1)} \\ \Delta W_{ij}^{(l-1)} = -\eta \frac{\delta E_{jk}^{(l)}}{W_{ij}^{(l-1)}} \end{cases} \tag{5}$$

Here, η represents the learning rate, and $0 < \eta < 1$.

Comprehensive (1) to (3) get:

$$\frac{\delta E_{jk}^{(l)}}{\delta W_{ij}^{(l-1)}} = \frac{\delta E_{jk}^{(l)}}{\delta O_{jk}^{(l)}} \frac{\delta O_{jk}^{(l)}}{\delta I_{jk}^{(l)}} \frac{\delta I_{jk}^{(l)}}{\delta W_{ij}^{(l-1)}} = \delta_{jk}^{(l)} \frac{\delta I_{jk}^{(l)}}{\delta W_{ij}^{(l-1)}} = \delta_{jk}^{(l)} O_{ik}^{(l-1)} \tag{6}$$

(2) Methods and steps for BP neural network fault diagnosis

In general, for a mechanical system, when different faults occur, the traits exhibited are different, and the corresponding characteristic parameters will also change. Therefore, there is a certain functional relationship between the cause of the fault and the characteristic parameters. In general, this relationship is non-linear. Therefore, the BP neural network's powerful nonlinear approximation ability can be used to identify various fault types.

According to the construction principle of the Boolean matrix, there are m characteristic parameters in the fault diagnosis, namely $G = (s_1, s_2, \cdots s_m)$, and there are n fault types to be identified, which is $C = (r_1, r_2, \cdots r_n)$. According to fuzzy clustering analysis, r_i takes a value between 0 and 1. It is determined that the largest degree of membership in r_i is the cause of component failure. The design of the BP neural network begins after determining the input and output vectors of the fault diagnosis system. The design of BP network mainly includes the selection of the number of network layers, the determination of the number of hidden layer neurons, the initialization of weights and the selection of learning steps. When using BP neural network to achieve specific fault diagnosis, the extracted feature vectors can be divided into two groups. One is as a training sample and the other is used as a test sample to verify the correctness of the network training. Therefore, the general steps of BP neural network fault diagnosis are shown in Fig. 1.

2.2. Adaptive fuzzy neural network ANFIS

The network-based adaptive fuzzy inference system ANFIS is also called adaptive neural fuzzy inference system, which is a product of network learning type combination. The ANIFS fuzzy neural network fault diagnosis system realizes the organic combination of fuzzy classification and neural network. It constructs a fuzzy inference system using a given input and output data set, and uses a separate backpropagation algorithm or a combination of the algorithm and the least squares method to adjust the parameters of the system membership function. This allows the fuzzy system to learn information from its modeling data rather than arbitrarily based on experience or intuition. For those rotating mechanical devices whose characteristics are not fully understood or have very complicated characteristics, fault diagnosis can still be performed, which solves the problem that the fuzzy inference application object is restricted, and also makes the parameters of the neural network have certain practical significance.

(1) ANFIS structure

For ease of explanation, it is assumed that the ANFIS system using the Takagi-Sugeno-type fuzzy rule has two inputs x and y, one output z, and contains the following two rules:

$$\begin{cases} \text{if } x \text{ is } A_1 \text{ and } y \text{ is } B_1, \text{ then } f_1 = a_{1x} + b_{1y} + c_1 \\ \text{if } x \text{ is } A_2 \text{ and } y \text{ is } B_2, \text{ then } f_2 = a_{2x} + b_{2y} + c_2 \end{cases} \tag{7}$$

The corresponding ANFIS structure is shown in Fig. 2. The connection between nodes only represents the flow of signals. No weight is associated with it: a square node represents a node with tunable parameters. A circular node represents a node without tunable parameters. Among them, only the first layer and the fourth layer have tunable parameters.

The functions of each layer are as follows:

The first layer: the input variable is fuzzified, and the membership degrees of x and y on the fuzzy subsets A_1 and B_1 are obtained. The output is:

$$O_j^l = \mu_{A_i}(x) \tag{8}$$

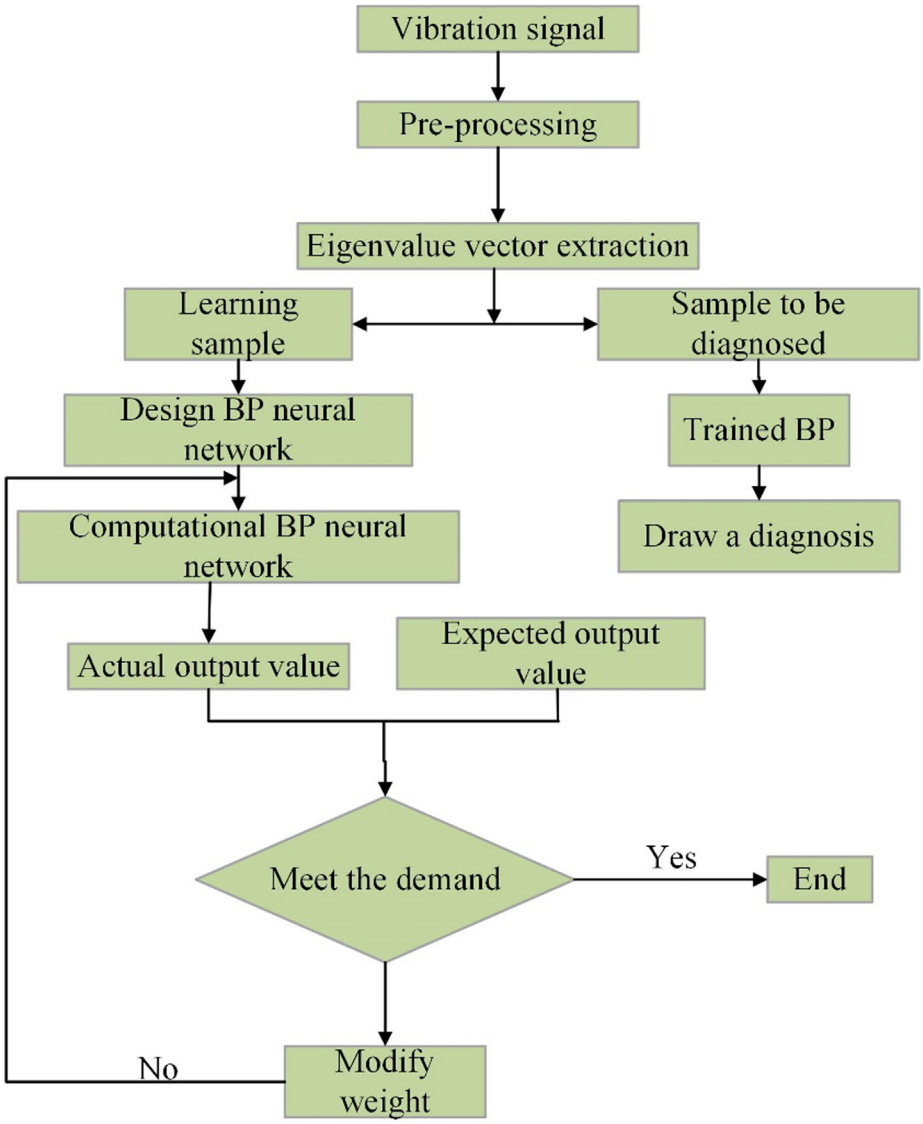

Fig. 1. BP neural network troubleshooting steps.

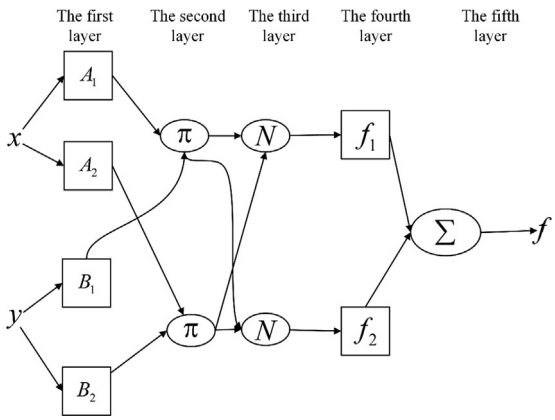

Fig. 2. ANFIS structure diagram.

According to the selected membership function form, the corresponding parameter set can be obtained, which is called the predecessor parameter. For example, if a commonly used Gaussian membership function is selected, then all $\{\sigma_I, d_i\}$ in equation (8) constitute the set of predecessor parameters. During the sample learning process, ANFIS can adaptively adjust the value of each parameter.

$$\mu_{A_i}(x) = \exp\left[-\frac{||x-d||_i^{\,2}}{\sigma_i^2}\right] \tag{9}$$

The second layer: the output is the product of the input signal, which means the activating strength of the sample to the rule.

$$O_i^2 = w_i = \mu_{A_i}(x) \times \mu_{B_i}(y) \tag{10}$$

The third layer: normalizes the activation intensity of each rule.

$$O_i^3 = \bar{w_i} = \frac{w_i}{w_1 + w_2} \tag{11}$$

The fourth layer: defuzzing the operation node, each node calculates the output of the corresponding rule.

$$O_i^4 = \bar{w_i} f_i = \bar{w_i}\,(a_i x + b_i y + c_i) \tag{12}$$

The set of parameters consisting of all $\{a_i, b_i, c_i\}$ is called the post-parameter parameter set.

Layer 5: Calculate the sum of the outputs of all rules:

$$O_i^4 = f = \sum_i \bar{w_i} f_i = \frac{\sum_i w_i f_i}{\sum_i w_i} \tag{13}$$

It can be seen from the structure of ANFIS that ANFIS is equivalent to a fuzzy inference system. Using neural network structure, fuzzy reasoning has the ability of self-learning

The learning of ANFIS comes down to the adjustment of the antecedent parameters (non-linear parameters) and the post-component parameters (linear parameters). For the predecessor parameters of (8) and the post-parameters of (11), according to the relationship between input and output, BP algorithm (backpropagation algorithm) and least squares estimation algorithm are used to adjust parameters, which is called hybrid algorithm. One iteration of the hybrid learning algorithm consists of two steps: the first step is to fix the parameters of the antecedent, and the input signal is passed along the network to the 4th layer, and the least squares estimation algorithm is used to adjust the parameters of the latter. After that, the signal continues to pass along the network forward until the output layer (ie, layer 5). In the second step, the obtained error signal is propagated back in the network, and the BP algorithm is used to adjust the parameters of the antecedent. Using the hybrid learning algorithm, for the given antecedent parameters, the global best of the post-parameter parameters can be obtained, which not only reduces the dimension of the search space in the gradient descent method, but also greatly improves the convergence speed of the parameters.

(2) Implementation of ANFIS-based rotating machinery fault diagnosis method

The mass imbalance, oil film whirl and normal eigenvector samples obtained by wavelet packet decomposition are used as training samples (10 training samples are selected for each working condition). The standard output of the network is {1} when the rotating machine is in normal operation, {2} when the mass is unbalanced, and the standard output of the network is {3} when the oil film is whirl. The membership function of the input variable is uniformly taken as the gauss function, and the number of membership functions is taken as 2. The function ANFIS is used to obtain a fuzzy system model that conforms to the original input and output data.

The obtained fuzzy system model is trained by training samples. During the training process, ANFIS can adaptively construct fuzzy sets and fuzzy rules according to the samples and given related parameters, and adjust the parameters of the membership function. The change of the membership function curve of the input variables before and after identification fully reflects the self-learning ability of the fuzzy neural network (ANFIS). After the network training is completed, the test samples are input into the trained neural network for fault diagnosis. In this paper, the remaining rotating mechanical mass imbalance, oil film whirl and normal feature vector are taken as test samples (11 test samples are selected for each working condition, which is different from the training samples). Input ANFIS fuzzy neural network for fault diagnosis. The correct diagnosis rate of the measured samples of the fault reached 82%. This is much higher than the neural network, indicating that this method combined with wavelet and ANIFS can effectively diagnose the rotating machinery.

3. Experiments

In the diagnosis of rotating machinery faults, the first layer of the multi-layer diagnostic network acts as the symptom layer $X = [x_{1p}, x_{2p}, \ldots\ldots x_{np}]$. Each symptom element x_{ip} corresponds to a neuron input by the network. The last layer corresponds to the output layer $Y = [y_{1p}, y_{2p}, \ldots\ldots y_{np}]$ of various fault classifications. The fault element yip corresponds to the neuron output by the network. The hidden layer is used to input high-order correlation features in the signal to form a diag-

nostic model of the multi-layer structure. p is the sample number, $p = 1, 2, \cdots, N$, learning learning rate and dynamic factor are determined experimentally. In the process of fault diagnosis of rotating machinery, the frequency domain characteristics of the vibration signal are taken as symptoms of failure. In this case, according to the symptom score table of Dr. Bai Muwan and others who have studied for many years, it is shown that $(0.01 \sim 0.39)f$, $(0.40 \sim 0.49)f$, $(0.51 \sim 0.99)f$, $1f$, $3f$, $(3 \sim 5)f$, odd-numbered f, high-frequency and other 9 representative frequency components are used as characteristic frequencies, and their corresponding spectral values are used as fault signs. 9 typical faults that occur more frequently in the field are selected for analysis. Fault types include initial imbalance, bumping, misalignment, bearing and journal eccentricity, spin crack, coupling failure, structural resonance, oil film oscillation, and looseness. The frequency domain indication of the above fault types is used as an input sample of the BP diagnostic network for the training section. The corresponding fault target output 1 represents fault and 0 represents no fault.

The experimental network selected by the experiment has 9 input layer nodes, 10 intermediate layer nodes, and 9 output layer nodes. The learning factor $\eta = 9.0$ and the dynamic factor $\alpha = 0.5$. The neural network learning sample input is shown in Table 1. The values in the table represent the eigenvalue size of the training instance, and the value interval is $[0 \sim 1]$. For example, in the first sample training example, its $(0.01 \sim 0.39)f$ represents an equivalent value of 0.01 to 0.39 octave vibration amplitude of $0.1f$ indicates that the equivalent value of the 1 octave vibration amplitude is 0.9. The rest are analogous. Therefore, the whole training process is essentially to extract the statistical characteristics of the training sample set.

In artificial neural networks, learning is an algorithm that corrects weights to obtain appropriate mapping functions or other system performance. The target output of the network is $\{0, 0, \cdots y_i, 0, 0, \cdots, 0\}, y_i = 1$, $i = 1 \sim 9$ represents the ith of the above nine faults. Using this sample to train the network, you can get the neural network you need. However, the actual network output value is close to 1, not exactly equal to 1. Although there is an error, it is negligible in practice.

4. Discussion

The normal samples of the rotating machine and the feature vectors of the two fault samples were input into the neural network and the fuzzy classification system respectively for fault diagnosis (again 19 samples for each working condition, 8 for training and 11 for testing). The diagnosis results were compared with the diagnosis results of ANFIS. The comparison results are shown in Table 2.

From the comparison of the diagnostic results in Table 2, we can see that ANFIS has more accurate diagnostic accuracy and superior performance than neural network and fuzzy classification system. It can easily realize complex reasoning in fault diagnosis, making the whole reasoning system structurally efficient and accurate.

4.1. Experimental analysis of rotor imbalance failure

In order to facilitate the installation of the rotor weight screw, a circumferential balance groove is machined on both sides of the turntable, the radius is $R = 33mm$, and the two scales are correspondingly engraved with the same scale, which facilitates the position selection of the counterweight screw. The counterweight screw is a standard M2 screw with a mass of approximately 0.3 g. Install 1 to 3 counterweight screws at a certain angle of the rotor to make the rotor unbalanced to simulate the rotor imbalance fault, and install the number of counterweight screws to control the severity of the fault.

In order to avoid the adverse effects of the severe vibration at the critical speed on the test bench, the experiment is not selected at a speed close to the critical speed. The speeds selected for this experiment were 3500r/min, 4500r/min and 5500r/min. Fig. 3 shows the time domain waveform and spectrum of an unbalanced fault. As can be seen from Fig. 3, the waveform is approximately sinusoidal. In the spectrogram, except for the fundamental frequency (rotational frequency), basically no other frequency components exist. Fig. 4 shows the spectrum of the unbalanced fault signal at three different speeds. The speeds are 3450r/min, 4533r/min, and 5619r/min (more than the first-order critical speed). By observing the amplitude of the fundamental frequency in each spectrogram, it can be seen that before the critical speed, the amplitude of the vibration increases with the increase of the speed, and the amplitude reaches the maximum value at the critical speed. When the critical speed is exceeded, the vibration amplitude will decrease rapidly and then increase slowly. The energy spectrum of the unbalanced fault signal extracted by the harmonic wavelet packet technique and normalized, it can be seen that the energy is mainly concentrated in the second frequency band. The frequency corresponding to the second frequency band is the fundamental frequency, indicating that the frequency component of the signal is importantly distributed near the fundamental frequency, which is consistent with the frequency distribution in the spectrogram.

4.2. Experimental analysis of rotor misalignment failure

Loosen the fixing bolts of the bearing support at one end of the rotating shaft, place 1 or 2 small washers under the support, and then tighten the bolts, that is, raise one end of the rotor so that the rotating shaft is inclined at an angle with respect to the motor shaft. Simulated rotor misalignment test. If the rotor is misaligned, it will generate a torque on the shaft. If the amplitude is too large, it will cause a certain degree of damage to the shaft. Therefore, only the speed before the first-order critical speed is selected for testing. The rotational speeds selected in this experiment were 3000 r/min, 3500 r/min and 4000 r/min. Fig. 5 is a time domain waveform and spectrum diagram of the rotor misalignment fault signal. It can be seen that the

Table 1
Neural network input samples of the spectrum sign of rotating machinery.

Spectrum indication		Sample number								
		1	2	3	4	5	6	7	8	9
1	$(0.01 \sim 0.39)f$	0	0.1	0	0	0	0.1	0	0	0
2	$(0.40 \sim 0.49)f$	0	0.1	0	0	0	0.2	0	0.1	0.1
3	0.5f	0	0.1	0	0	0	0	0.1	0	0.2
4	$(0.51 \sim 0.99)f$	0	0.1	0	0	0	0.1	0.1	0	0
5	1f	0.9	0.2	0.4	0.8	0.4	0.2	0	0	0
6	2f	0.05	0.1	0.5	0.2	0.6	0.3	0	0	0
7	$(3 \sim 5)f$	0.05	0.1	0	0	0	0.1	0	0	0
8	Odd number f	0	0.1	0	0	0	0	0	0	0.1
9	High frequency	0	0.1	0	0	0	0	0	0	0

Table 2
Comparison of diagnostic methods for various identification methods.

Method	Normal status Number of samples (19)		Oil film oscillation Number of samples (19)		Unbalanced quality Number of samples (19)		Diagnostic result Number of samples (57)		Accuracy
	Training	Test	Training	Test	Training	Test	Training	Test	
NN	8	11	8	11	8	11	24	33	0.70
Fuzzy Model	_	11	_	11	_	11	_	33	0.66
ANFIS	8	11	8	11	8	11	24	33	0.79

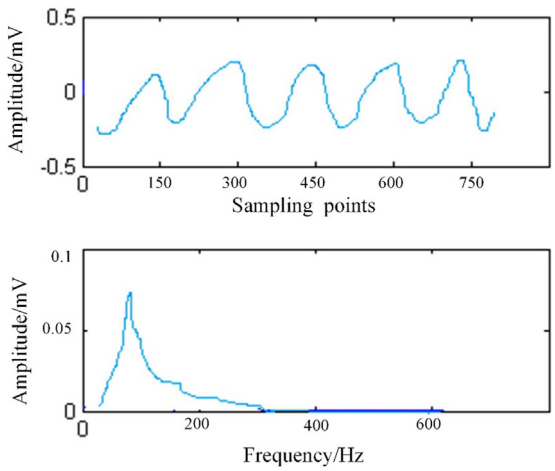

Fig. 3. Time domain waveform and spectrogram of unbalanced fault.

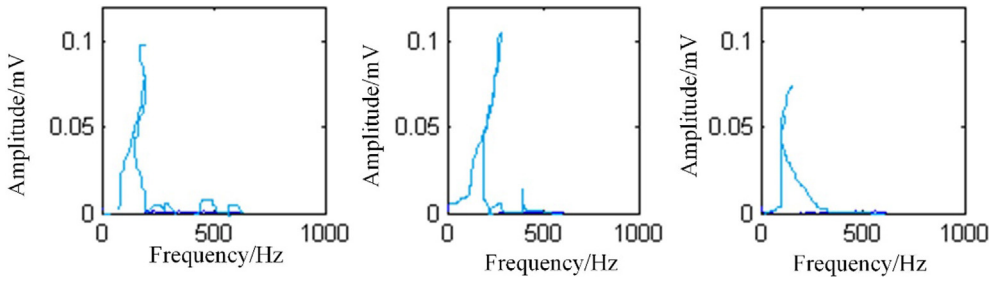

Fig. 4. Unbalanced fault spectrum at different speeds.

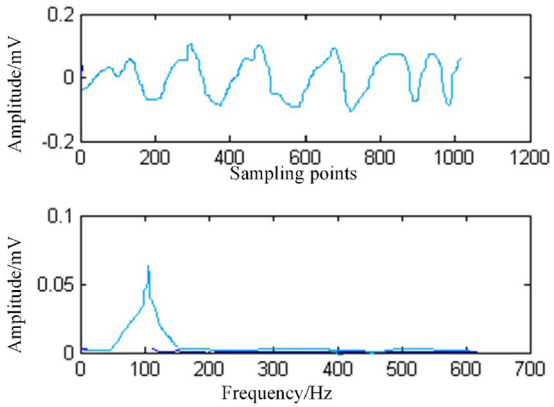

Fig. 5. Time domain waveform and spectrogram of misalignment.

main spectrum of the misalignment fault is characterized by the presence of 1 octave and 2 octave components, accompanied by a slight high order even octave. Through multiple tests at different speeds and different degrees of failure, it is found that as the degree of failure increases, the proportion of the 2 octave component also increases. The energy spectrum of the misaligned fault signal calculated by the harmonic wavelet packet decomposition can be used to more clearly see the existence of the 1x and 2x components and their proportion.

4.3. Experimental analysis of dynamic and static rubbing faults

Install the rubbing screw on the rotating shaft near the turntable, and gradually close the rubbing screw to the rotating shaft, but do not touch it completely. As the rotational speed of the rotor gradually increases, the amplitude of the vibration becomes larger and larger under the action of the unbalanced force. When the distance between the rotating shaft and the rubbing screw is reached or exceeded, a collision will occur between the rotating shaft and the rubbing screw to simulate the dynamic and static rubbing fault of the rotor. Multiple tests were performed by varying the rotor speed, rotor imbalance, and the distance between the shaft and the rubbing screw. Because the impact of the screw and the rotating shaft in the experiment will cause damage to the rubbing and rotating shaft, it is the same as the misalignment, and only the speed before the first critical speed is selected for testing. The rotational speeds selected for this experiment were also 3000 r/min, 3500 r/min and 4000 r/min. Fig. 6 shows the time domain waveform and spectrum of the dynamic and static rubbing fault. It can be seen from the figure that the spectral characteristics of the rubbing fault are mainly characterized by 1x, 2x, 3x, 4x and some weaker higher frequency multipliers. And as the multiple increases, the amplitude gradually decreases. Through multiple sets of data analysis, it is known that as the rubbing increases, the amplitude of the 1 octave component is reduced, and the other doubling components are slightly increased. Through the energy spectrum corresponding to Fig. 6, the existence and proportion of each frequency doubling component are more intuitively explained.

4.4. Experimental analysis of oil film eddy failure

A special bearing for oil film eddy test and a special shaft with a shoulder are mounted on the rotor test stand. The turntable is placed at 1/3 of the axial length of the inner bearing housing, and an oil cup is placed above the special bearing housing. Before the motor starts, open the oil cup and open the motor to simulate the oil film whirl failure until the oil in the oil film bearing flows out. The experimental speeds were 2000 r/min, 3000 r/mi, 4000 r/min and 5000 r/min. Fig. 7 and Fig. 8 are time-domain waveforms, spectrograms and energy spectra of vibration signals in a typical rotor oil film whirl failure. From the energy spectrum and the spectrogram, the existence of the 1/2 frequency component can be clearly seen, and the proportion of the 1/2 frequency component is very high, indicating that the degree of oil film eddy failure of the rotor is very serious.

Fig. 9 is a signal spectrum diagram of oil film whirl failure at different speeds. The rotational speed of Fig. 9a) is 1941 r/min. It can be seen from the figure that almost no 1/2 octave component exists, and only a small protrusion can be seen, mainly based on 1 octave. This means that at 1941r/min, the rotor did not occur or only a slight oil film whirl failure. The rotation speed of Fig. 9b) is 3083r/min, and the presence of the 1/2 frequency component can be clearly seen at this time, but the amplitude is small compared with the 1 octave component. This indicates that a slight oil film whirl failure is occurring in the rotor. The rotational speed of Fig. 9c) is 4040 r/min. It can be seen from the figure that the amplitude of the 1/2 octave component exceeds the octave component. This indicates that a serious oil film whirl failure has occurred at this time. The rotation speed of Fig. 9d) is 4970r/min, and all the frequency components except the 1/2 frequency component are almost invisible in the spectrogram. This phenomenon indicates that the rotor is completely in the oil film whirl state.

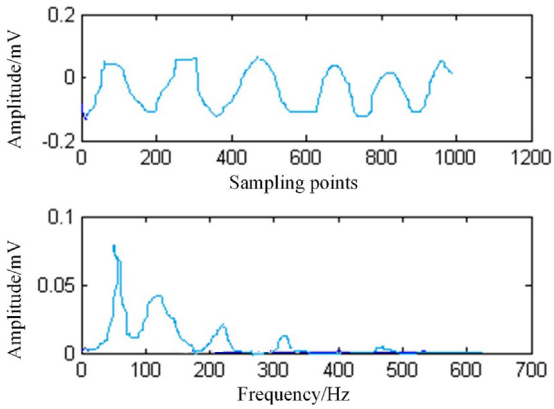

Fig. 6. Time domain waveform and spectrogram of dynamic and static rubbing fault.

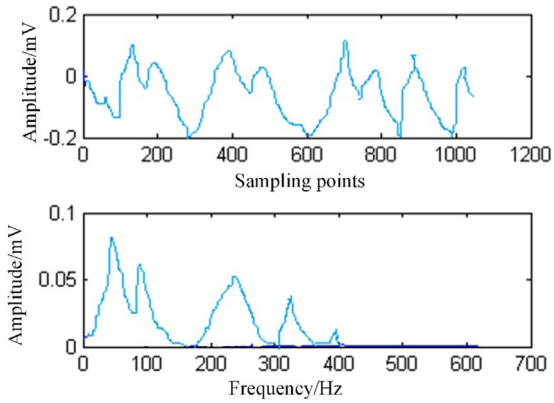

Fig. 7. Time domain waveform and spectrogram of oil film eddy failure.

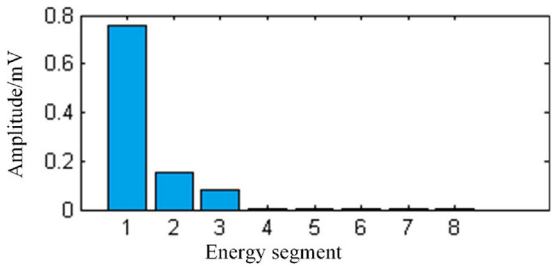

Fig. 8. Energy spectrum of oil film eddy failure signal.

5. Conclusions

In this paper, the integrated signal processing technology and intelligent fault diagnosis technology have systematically and deeply studied the methods of signal processing and intelligent fault diagnosis and its application in vibration signal processing and fault diagnosis of rotating machinery, and obtained the following results:

(1) The feature extraction method of rotating machinery vibration signal is studied. According to the time-varying characteristics of the rotating machinery vibration signal and the difficulty of extracting the characteristics, the wavelet transform function selection principle and the soft threshold principle of wavelet packet denoising are proposed by further research on wavelet transform technology. The denoising processing and feature extraction of the rotating machinery vibration signal are performed by wavelet packet transform. With the "energy" as the element, the char-

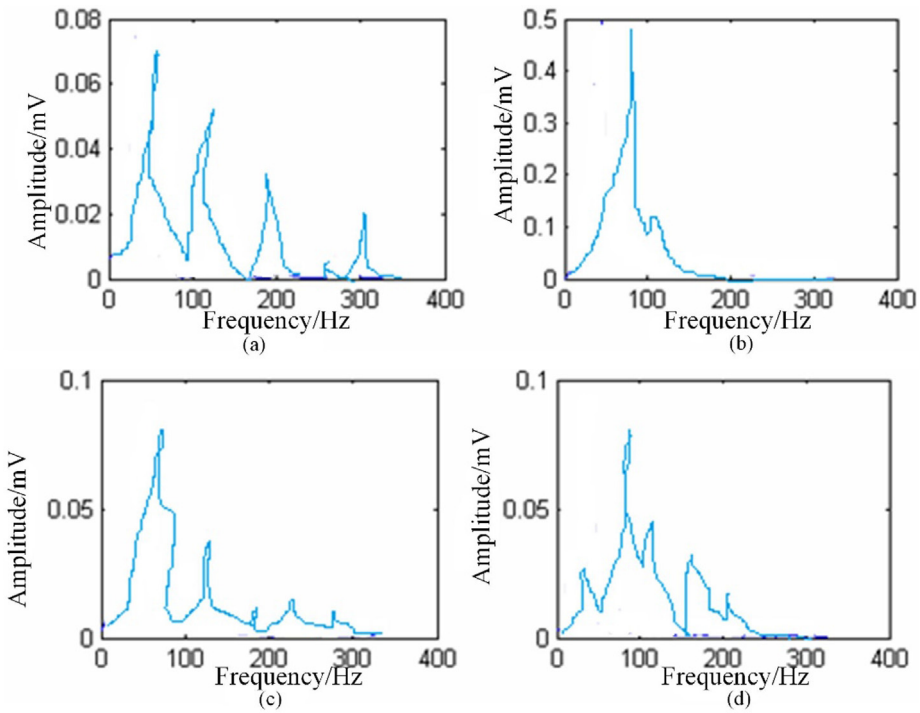

Fig. 9. Oil film eddy signal spectrum at different speeds.

acteristic vector of the rotating mechanical vibration signal is constructed, which provides a convenient processing method for the fault feature extraction of the rotating machinery vibration signal and the subsequent fault intelligent diagnosis. The vibration signal analysis results of unbalanced rotating machinery and oil film eddy failure further verify the feasibility and effectiveness of this method.

(2) The fault diagnosis methods of neural networks and fuzzy systems are studied. Fuzzy systems lack self-learning ability. The selection of membership function and fuzzy rules is subjective and dependent on experts. The input/output relationship obtained by neural networks cannot be expressed in an easily accepted way. His absoluteness makes the diagnosis result inconsistent with the actual situation. Aiming at the above shortcomings, through the research on the combination of neural network and fuzzy system, a fuzzy neural network (NAFIS) based fault diagnosis method for rotating machinery is proposed and used for fault diagnosis of rotating machinery. The experimental results show that compared with the commonly used neural network and fuzzy system diagnosis methods, this method can make up for the shortcomings of fuzzy and neural network alone, and has higher diagnostic accuracy. It has a good application prospect in the field of fault diagnosis of rotating machinery.

(3) Based on the in-depth analysis of the fault diagnosis process of rotating machinery, with the powerful MATLAB language system and its toolbox, the development and design of the prototype software for rotating machinery fault diagnosis is completed in this paper, and the common faults of rotating machinery are used. The eigenvector data of the state is tested for the correctness of the diagnosis results, and the effect is good, which proves the availability of the system.

CRediT authorship contribution statement

Xianzhen Xu: Conceptualization, Methodology. **Dan Cao:** Data curation, Writing - original draft. **Yu Zhou:** Visualization, Investigation. **Jun Gao:** Software, Validation.

Declaration of Competing Interest

The authors declare that they have no known competing financial interests or personal relationships that could have appeared to influence the work reported in this paper.

Appendix A. Supplementary data

Supplementary data to this article can be found online at https://doi.org/10.1016/j.ymssp.2020.106625.

References

[1] J. Jang, C. Ha, B. Chu, J. Park, Development of fault diagnosis technology based on spectrum analysis of acceleration signal for paper cup forming machine, J. Korean Soc. Manuf. Process Eng. 15 (6) (2016) 1–8.
[2] S. Deng, L. Tang, X. Su, J. Che, Fault diagnosis technology of plunger pump based on EMMD-teager, Int. J. Performability Eng. 15 (7) (2019) 1912.
[3] A. Graves, G. Wayne, M. Reynolds, T. Harley, I. Danihelka, A. Grabska-Barwińska, A.P. Badia, Hybrid computing using a neural network with dynamic external memory, Nature 538 (7626) (2016) 471.
[4] J. Zbontar, Y. LeCun, Stereo matching by training a convolutional neural network to compare image patches, J. Mach. Learn. Res. 17 (1–32) (2016) 2.
[5] K.H. Jin, M.T. McCann, E. Froustey, M. Unser, Deep convolutional neural network for inverse problems in imaging, IEEE Trans. Image Process. 26 (9) (2017) 4509–4522.
[6] M.A. Anderson, J.E. Burda, Y. Ren, Y. Ao, T.M. O'Shea, R. Kawaguchi, M.V. Sofroniew, Astrocyte scar formation aids central nervous system axon regeneration, Nature 532 (7598) (2016) 195.
[7] A.I. Seixas, M.M. Azevedo, J.P. de Faria, D. Fernandes, I.M. Pinto, J.B. Relvas, Evolvability of the actin cytoskeleton in oligodendrocytes during central nervous system development and aging, Cell. Mol. Life Sci. 76 (1) (2019) 1–11.
[8] H. Wu, X.H. Wang, B. Gao, N. Deng, Z. Lu, B. Haukness, H. Qian, Resistive random access memory for future information processing system, Proc. IEEE 105 (9) (2017) 1770–1789.
[9] M. Guillaume, S. Handgraaf, A. Fabre, I. Raymond-Letron, E. Riant, A. Montagner, H. Guillou, Selective activation of estrogen receptor α activation function-1 is sufficient to prevent obesity, steatosis, and insulin resistance in mouse, Am. J. Pathol. 187 (6) (2017) 1273–1287.
[10] D.B. Xu, S.Q. Gao, Y.N. Ma, X.T. Wang, L. Feng, L.C. Li, Y.Z. Ma, The G-protein β Subunit AGB1 promotes hypocotyl elongation through inhibiting transcription activation function of BBX21 in arabidopsis, Molecular Plant 10 (9) (2017) 1206–1223.
[11] A. Wanto, A.P. Windarto, D. Hartama, I. Parlina, Use of binary sigmoid function and linear identity in artificial neural networks for forecasting population density, Int. J. Inf. Syst. Technol. 1 (1) (2017) 43–54.
[12] R. Xu, M. Zhou, Sliding mode control with sigmoid function for the motion tracking control of the piezo-actuated stages, Electron. Lett. 53 (2) (2016) 75–77.
[13] M. Anthimopoulos, S. Christodoulidis, L. Ebner, A. Christe, S. Mougiakakou, Lung pattern classification for interstitial lung diseases using a deep convolutional neural network, IEEE Trans. Med. Imaging 35 (5) (2016) 1207–1216.
[14] Z. Wang, S. Joshi, S. Savel'ev, W. Song, R. Midya, Y. Li, H. Jiang, Fully memristive neural networks for pattern classification with unsupervised learning, Nat. Electron. 1 (2) (2018) 137.
[15] Xinjun Peng, A spheres-based support vector machine for pattern classification, Neural Comput. Appl. 31 (S-1) (2019) 379–396.
[16] Gu. Nannan, Pengying Fan, Mingyu Fan, Di Wang, Structure regularized self-paced learning for robust semi-supervised pattern classification, Neural Comput. Appl. 31 (10) (2019) 6559–6574.
[17] Z. Kovács, F. Szelecsényi, K. Brezovcsik, Preparation of thin gadolinium samples via electrodeposition for excitation function studies, J. Radioanal. Nucl. Chem. 307 (3) (2016) 1861–1864.
[18] M.S. Uddin, K.S. Kim, M. Nadeem, S. Sudár, G.N. Kim, Excitation function of alpha-particle-induced reactions on nat Ni from threshold to 44 MeV, Eur. Phys. J. A 53 (5) (2017) 100.
[19] T. Ren, S. Liu, G. Yan, H. Mu, Temperature prediction of the molten salt collector tube using BP neural network, IET Renew. Power Gener. 10 (2) (2016) 212–220.
[20] Z. Zhao, Q. Xu, M. Jia, Improved shuffled frog leaping algorithm-based bp neural network and its application in bearing early fault diagnosis, Neural Comput. Appl. 27 (2) (2016) 375–385.
[21] N.J. Guliyev, V.E. Ismailov, A single hidden layer feedforward network with only one neuron in the hidden layer can approximate any univariate function, Neural Comput. 28 (7) (2016) 1289–1304.
[22] L. Lacasa, I.P. Mariño, J. Miguez, V. Nicosia, É. Roldán, A. Lisica, J. Gómez-Gardeñes, Multiplex decomposition of non-Markovian dynamics and the hidden layer reconstruction problem, Phys. Rev. X 8 (3) (2018) 031038.

Xianzhen Xu was born in Qingdao, Shandong, P.R. China, in 1988. He received the bachelor's degree from Ocean University of China, P.R. China. Now, he works in College of Chemical Science and Engineering, Qingdao University. His research interest include chemical engineering, computational chemistry, and data analysis.

Dan Cao was born in Qingdao. Shandong, P.R. China, in 1991. She are receiving the bachelor's degree from Ocean University of China. P.R. China. Now, he works in College of Engineering, Ocean University of China, Qingdao 266100, China.

Yu Zhou was born in Weihai. Shandong, P.R. China, in 1987. He received the bachelor's degree from Tsinghua University, P.R. China. Now, he works in College of Chemical Science and Engineering, Qingdao University.

Jun Gao was born in Changyi. Shandong, P.R. China, in 1968. College of Chemical and Environmental Engineering, Shandong University of Science and Technology, Qingdao 266590, China.